RSC Advances

ROYAL SOCIETY OF CHEMISTRY

www.rsc.org/advances

Tunable Morphologies of Indium Tin Oxide Nanostructures Using Nanocellulose Templates

Yuan Lu[§†*], *Joseph E. Poole II*[§†], *Tolga Aytug*[‡], *Harry M. Meyer III*[§], *and Soydan Ozcan*[§]

[†]The authors have made equal contributions to the work.
[*]Address correspondence to Dr. Yuan Lu, email: yuan.lv@gmail.com

[§] Materials Science and Technology Division, Oak Ridge National Laboratory, 1 Bethel Valley Road, Oak Ridge, TN. 37831
[‡]Chemical Sciences Division, Oak Ridge National Laboratory, 1 Bethel Valley Road, Oak Ridge, TN. 37831

Keywords: nanocellulose, indium tin oxide, controlled morphology, metal oxide, thin film

Abstract

Metal oxide nanostructures have emerged as an important family of materials for various device applications. The performance is highly dependent on the morphology of the metal oxide nanostructures. Here we report a completely green approach to prepare indium tin oxide (ITO) nanoparticles using only water and cellulose nanofibril (CNF) in addition to the ITO precursor. Surface hydroxyl groups of the CNFs allow for efficient conjugation of ITO precursors (e.g., metal ions) in aqueous solution. The resulting CNF film allows for controllable spatial arrangement of metal oxide precursors, which results in tunable particle morphology (e.g., nanowires, nanospheres, and octahedral nanoparticles). These ITO nanoparticles can also form conductive and transparent ITO films. This work opens a new perspective on developing metal oxide nanostructures.

Introduction

Size- and shape-controlled synthesis of monodispersed metal oxides has become increasingly important in novel microsystems and nanosystems for electronic, biomedical, and catalytic applications. Here we report an environmentally friendly, high-volume synthesis of controlled morphology indium tin oxide (ITO) nanoparticles. The unique properties of ITO (e.g., high electrical conductivity and high optical transparency) have driven this material to become one of the industrial standards among transparent conductive oxides. ITO has been used in many modern devices such as photovoltaic cells, flat panel displays, light-emitting diodes, biomolecular microarrays, and toxic-gas sensors, all of which are growing in demand.[1-7] Recently, ITO nanoparticles have received tremendous interest in areas demanding porous electrodes and enhanced performance of electrochemical capacitors, solar cells, and lithium ion batteries.[8-13] Other advantages include low manufacturing cost and adaptability to various substrate materials and geometries in thin film form.[14] The morphology and size of ITO nanoparticles have been demonstrated to determine the properties exhibited in ITO products.[15-17] As a result, several methods have been developed for preparing ITO nanoparticles including seed-layer-assisted chemical bath deposition, chemical vapor deposition, alumina-template-assisted synthesis, solvothermal synthesis, coprecipitation, laser-induced fragmentation, microwave-assisted synthesis, and emulsion techniques.[18-25] However, the complexity of the aforementioned procedures leads to increased manufacturing cost and limits scalability. Additionally, these approaches cannot produce nanoparticles with tailored morphologies.

Recently, nanocellulose materials have been demonstrated to be great templates for synthesizing metal oxide nanotubes owing to their unique morphology and the ease of removal (e.g., high-temperature degradation).[26] Cellulose nanofibrils (CNFs) are nanosized

cellulose fibers with large numbers of surface hydroxyl groups produced by bacteria or derived from plants. Because of their extraordinary mechanical and optical properties, CNFs have been used as reinforcing fillers and in a variety of biomedical, industrial, and energy applications.[26-31] Previously, Korhonen, et al. reported the synthesis of metal oxide nanotubes using nanocellulose aerogel templates. An atomic layer deposition (ALD) technique was used to coat a layer of metal oxides onto the cellulose fibers. After annealing at a high temperature (e.g., 450°C), metal oxide nanotubes were yielded via the *in situ* removal of the nanocellulose templates.[26] However, this approach lacks the versatility of producing particles with tunable morphologies. Scalability of ALD may also be a hurdle for the commercialization of this technique.

Herein, we report a facile, scalable, and environmentally friendly approach to synthesize ITO nanoparticles using cellulose nanofibrils as a template. Different from ALD, we use the affinity of cellulose hydroxyl groups to metal ions to conjugate metal oxide (i.e., ITO) precursors in an aqueous environment. Unlike previous sol-gel synthesis of metal oxide nanoparticles[32, 33] where a solid gel is formed, the fibrous network of CNFs allows for the controllable distribution of metal ions localized on the nanofibers, thus resulting in tunable particle morphologies (e.g., nanowires, nanospheres, octahedrons). This approach was also adapted to prepare transparent ITO thin films. The nanocellulose-templating approach presented in this study provides a novel, simple, and scalable route to prepare ITO nanoparticles and thin films with tunable morphologies.

Methods

Materials. Reagent grade tin (II) chloride (98%) was purchased from the Aldrich Chemical Company (Milwaukee, Wisconsin). Indium trichloride (99.99%) was obtained from Indium Corporation (Clinton, New York). The cellulose nanofibril (CNF) suspension was a gift from the US Forest Product Laboratory. Commercially available indium tin oxide (ITO) nanoparticles (99.99%) were purchased from SkySpring Nanomaterials, Inc.

Synthesis of ITO nanoparticles. CNF stock solution (0.96 wt %) was prepared by diluting the as-received CNF solution by 10 fold. The ITO precursor stock solution was prepared by dissolving indium chloride (2.24 g) and tin chloride (0.21 g) in water (50 mL). An aliquot of the ITO precursor stock solution was diluted in 10 mL of water and added dropwise to 25 mL of CNF stock solution under stirring, followed by collection of the ITO precursor-conjugated CNFs by centrifugation. The CNFs were then redispersed in 10 mL of water and the resulting suspension was poured into a petri dish for film formation. After drying at room temperature for 24 h, the ITO-precursor-conjugated film was formed. This film was heated to 900°C in alumina boat at a rate of 10°C min^{-1} in a furnace to induce ITO particle formation and CNF removal.

Preparation of ITO coatings on glass. The ITO precursor stock solution was prepared by dissolving indium chloride (2.24 g) and tin chloride (0.21 g) in water (50 mL). An aliquot of the ITO precursor stock solution was added dropwise to 2.5 mL of CNF stock solution (0.96 wt %) under stirring, followed by collection of the ITO-precursor-conjugated CNFs by centrifugation. The CNFs were then redispersed in 1 mL of water and cast on a substrate for film formation. After drying at room temperature for 24 h, the ITO-precursor-conjugated film was formed. This film was placed on top of a glass slide and heated to 500°C at a rate of 10°C min^{-1} in a furnace and kepted at 500°C for 1 h to induce ITO particle formation and CNF removal. The resulting ITO coatings on glass slides were annealed under 4% hydrogen in argon at 350°C for 2 h prior to characterization.

Characterizations. Scanning electron micrographs were recorded with a Hitachi S-4800 scanning electron microscope (Pleasanton, California) to determine the size and morphology of the ITO particles and films. Powder x-ray diffraction patterns were collected on a PANalytical Empyrean diffractometer with Ni-filtered CuKα (λ=1.54Å) radiation operating at 45 kV and 40 mA. X-ray photoelectron spectroscopy analysis of the ITO particles was carried out with a Thermo Scientific K-Alpha x-ray photoelectron spectrometer equipped with a

conventional electron energy analyzer. The latter was operated in the fixed transmission mode at constant pass energy of 200 eV for the survey spectra and 50 eV for the core level spectra. A monochromatic Al Kα source (1,486.6 eV) operated at 420 W (14 kV; 30 mA) was used as incident radiation. Photo-emitted electrons were collected at a take-off angle of 90° from the sample and the pressure was about 10^{-7} Pa. The spectrometer energy scale was calibrated with respect to Ag 3d5/2, Au 4f7/2, and Cu 2p3/2 core level peaks, set with binding energies of 368.3, 84.0, and 932.7 eV, respectively. For elemental quantification, the accuracy of the analysis was considered to be ±1%. The resistivity, carrier mobility, and carrier concentration of the films were estimated by Hall measurements (Ecopia HMS 3000), using the van der Pauw method, at room temperature with a field strength of 5.7 kG. The system includes software with I-V curve capability for checking the ohmic integrity of the user-made sample contacts. The sheet resistance was measured by a four-point probe technique.

Conjugation of In^{3+} and Sn^{2+} to CNFs. CNFs exhibit great affinity to positively charged metal ions due to the large number of hydroxyl groups on their surfaces. At high concentrations, metal ions can cross-link with CNFs to form a hydrogel. To confirm the conjugation of In^{3+} and Sn^{2+} with CNFs, ITO precursor solution was mixed with as-received CNF solution in a 1 : 1 mass ratio of CNF and ITO precursor (e.g., indium chloride and tin chloride). The addition of ITO precursors immediately resulted in gelation, as shown in Figure S1, confirming our hypothesis that In^{3+} and Sn^{2+} are able to efficiently conjugate to the CNF surfaces. Of note, this is simply a demonstration of the affinity of ITO precursors for the CNFs. In this study, diluted solutions were used to avoid premature cross-linking and gelation.

Results and Discussion

Preparation of ITO precursor-conjugated CNF films. A schematic illustration of the typical synthetic procedure is shown in **Figure 1**. ITO precursors (i.e., indium (III) chloride and tin (II) chloride) were dissolved in distilled water with an In : Sn molar ratio of 9 : 1. This ITO precursor solution was then added dropwise to the CNF suspension (0.1 wt %) (Figure

1a). The ITO precursors were expected to conjugate to the surface hydroxyl groups according to a previous report by Dong et al.[29] Indeed, multivalent cations were found to conjugate to the CNFs efficiently to form a cross-linked hydrogel.[29]

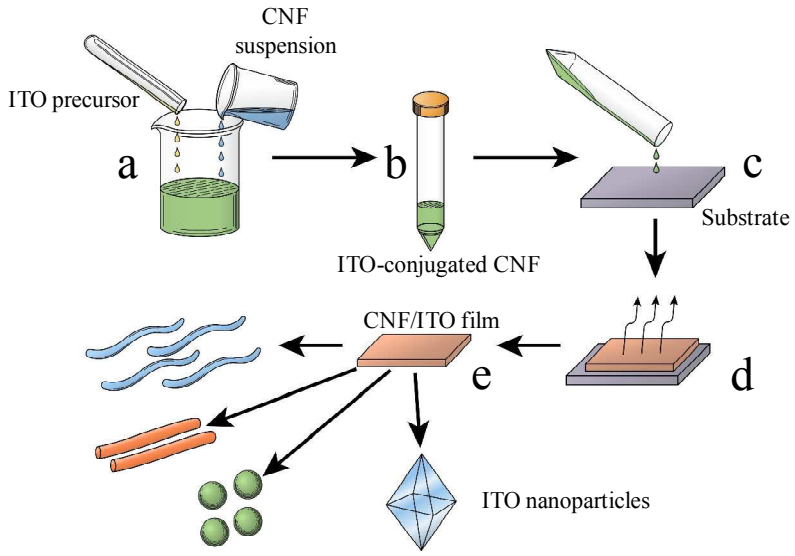

Figure 1. Schematic illustration of the synthesis of indium tin oxide (ITO) nanoparticles using cellulose nanofibril (CNF) templates: a, ITO precursor conjugation to CNF; b, collection of ITO-conjugated CNF by centrifugation; c, redispersion in water and casting onto a substrate; d, removal of the solvent to form a film; and e, annealing at high temperature to yield ITO nanoparticles.

Analogously, the same observation was also noted for the present case of ITO precursors (i.e., In^{3+} and Sn^{2+}), indicating a strong interaction with CNFs (Supporting Information Figure S1). To synthesize discrete nanoparticles, diluted solutions of the ITO precursor and CNF suspension were necessary to prepare metal-ion-conjugated CNFs. Using diluted solutions avoided the gelation and led to a suspension of ITO-precursor-conjugated CNFs. The resulting fibers were then collected by centrifugation (Figure 1b) to remove unbound metal ions and redispersed into water (Figure 1c). This aqueous suspension was cast onto a substrate and dried (Figure 1d) to form a CNF film conjugated with ITO precursors. By annealing the film at high temperature (Supporting Information), particles with tunable morphologies (e.g., nanowires, nanospheres, octahedrons) were synthesized (**Figure 2**). Of note, this approach is

a green approach to produce ITO nanoparticles since only water and CNF were required. The simplicity of this approach guarantees the greater scalability in contrast to the previously reported ALD technique.

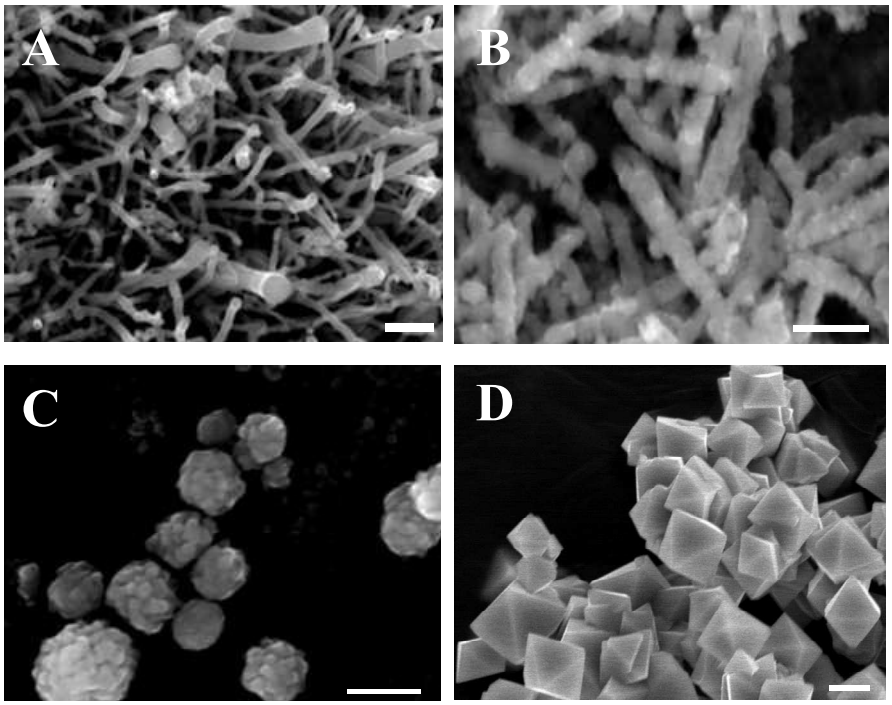

Figure 2. Scanning electron microscopy images of indium tin oxide (ITO) particles synthesized with a cellulose nanofibril : ITO precursor ratio of A, 1 : 5; B, 1 : 20; C, 1 : 30; and D, 1 : 80. Scale bar: 300 nm.

Effect of CNF/ITO ratio on the particle morphology. A range of mass ratios of CNF to ITO (CNF : ITO ratio) (i.e., 1 : 5, 1 : 20, 1 : 30, 1 : 80) was used to prepare the ITO-precursor-conjugated CNF because it is expected to have great influence on the spatial distribution of ITO precursors (**Figure 3**). For example, low ITO precursor doping levels may yield mostly the absorption of In^{3+} and Sn^{2+} on CNFs with minimal crosslinking between fibers (Figure 3A). Metal ions are locally concentrated on each CNF, but are far apart from those on different CNFs. Further increase in ITO precursor likely leads to an increase in the quantity of metal ions aggregated on the CNFs and the crosslinking sites between fibers (Figure 3B). As a result, the 3D distribution of metal ion clusters becomes less localized, indicating a decrease

in the spatial distance between metal clusters on neighboring CNFs. The extreme case of a large amount of excess ITO precursor is comparable to a saturated ITO precursor solution, characterized by a homogeneous distribution of metal ions (Figure 3C).

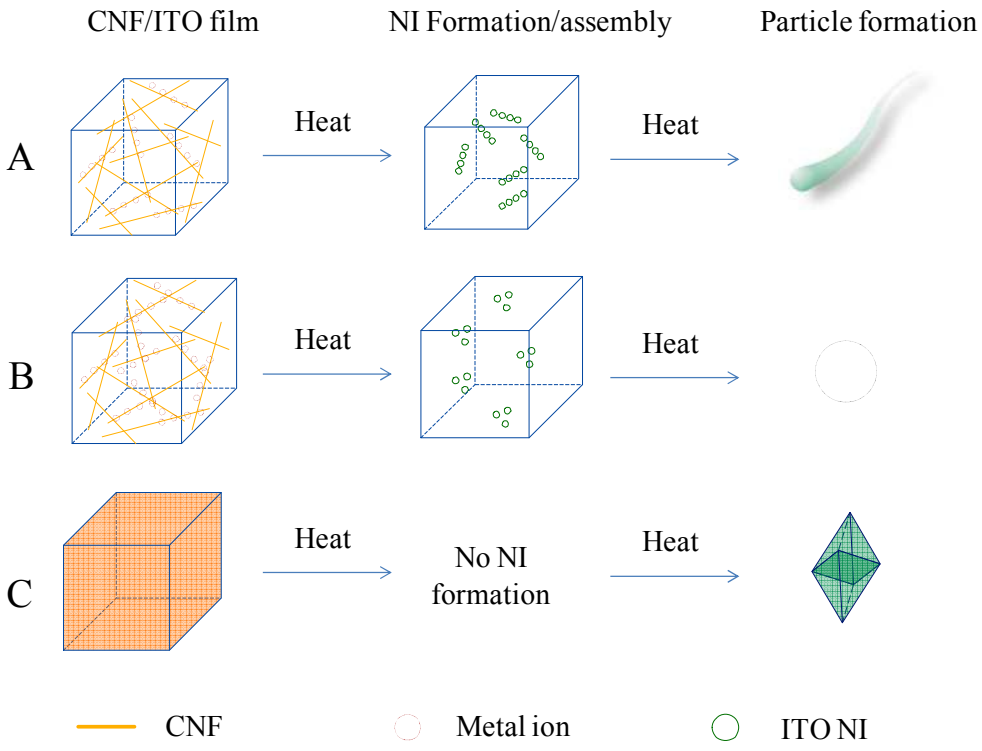

Figure 3. Proposed mechanism for the formation of various indium tin oxide (ITO) morphologies, using cellulose nanofibril (CNF) films as templates: A, nanowires; B, nanospheres; and C, octahedrons. NI: nanoislands.

As shown in Figure 2, the CNF : ITO ratio (or metal ion distribution) greatly affects particle morphology. When a CNF : ITO ratios of 1 : 5 and 1 : 20 are used, ITO nanowires or nanorods are produced. A CNF : ITO ratio of 1 : 20 was found to lead to greater surface roughness and particle diameter (**Table 1**).

Table 1. Identities of indium tin oxide (ITO) nanoparticles synthesized using cellulose nanofibril (CNF) templates

CNF : ITO	Morphology	Diameter (nm)[a]	Surface In : Sn
1 : 5	Nanowire	73 ± 5	81:19
1 : 20	Nanorod	107 ± 10	84:16
1 : 30	Nanosphere	268 ± 35	79:21
1 : 80	Octahedron	650 ± 65	82:18

Commercial ITO	-	-	87:13

[a]Particle size is determined by scanning electron microscopy images using ImageJ.

Further increase in the ITO precursor doping level (e.g., CNF : ITO ratio of 1 : 30) resulted in the formation of spherical particles with great surface roughness. In the most extreme scenario (e.g., CNF : ITO ratio of 1 : 80), the as-synthesized nanoparticles exhibited an octahedral structure. Unlike the other particles, these octahedral nanoparticles have smooth surfaces. X-ray diffraction patterns of the resulting particles match well with the cubic bixbyite peaks of commercial ITO nanoparticles, which are slightly shifted to higher 2θ values compared to those of pure cubic indium oxide (Figure 4).[14] The In : Sn ratio on the surface of these ITO particles was analyzed by x-ray photoelectron spectroscopy (Table 1). The atomic percentage of indium for the as-synthesized ITO particles is slightly lower than that for commercially available ITO particles, probably as a result of the well-documented volatility of indium at higher annealing temperatures (i.e., 900°C).[34]

The growth of the ITO thin films on a two-dimensional surface is known to follow the Volmer-Weber growth model.[35] Clusters of atoms are deposited and nucleate on the surface of the substrate forming isolated nanoislands (NIs). Further deposition results in growth of the NIs, which begin to impinge on each other, eventually coalescing to form a continuous film. Inspection of the morphology of ITO nanoparticles synthesized using CNF templates (e.g., CNF : ITO ratios of 1 : 5, 1 : 20, and 1 : 30) suggests the formation of NIs as evidenced by the hierarchical construction of smaller size individual islands on these particles. Indeed, as shown in Figures 2 and S2, particles generated from CNF : ITO ratios of 1 : 20 and 1 : 30 are evidently assemblies of NIs of ~ 30 nm in diameter. As a result, we propose a particle formation mechanism similar to the Volmer-Weber growth model. Clusters of metal ions are absorbed onto CNFs in aqueous solution. The resulting dried CNF films provide a controllable 3D distribution of metal ion clusters. Upon annealing, metal ion clusters sinter to form ITO NIs, accompanied by the simultaneous degradation and shrinkage of CNFs at high

temperature, which leads to the coalescing of NIs to form ITO nanoparticles. Therefore, the assembly of the NIs is a crucial step in determining particle morphology. Of note, the presence of CNFs between the ITO particles prevents further aggregation and coalescence, thus allowing for well-defined ITO nanoparticle formation with complete removal of the CNFs at high temperatures.

As shown in Figure 2, low-level ITO precursor concentrations within the CNF suspension (e.g., CNF : ITO ratios of 1 : 5 and 1 : 20) yielded ITO nanowires. In this scenario, most likely some CNFs may not have metal ions absorbed on their surfaces, isolating the metal ion clusters on one CNF from those on another, thus resulting in NIs (upon annealing) that are locally concentrated on individual CNFs (Figure 3A). The degradation and shrinkage of CNFs during annealing results in the coalescing of the neighboring NIs. The NIs preferentially assemble along the CNFs due to their accessibility and thus sinter to form a rod-like structure. As the CNF matrix continues to shrink, more NIs assemble along the rods, forming the ITO nanowires or nanorods. Of note, greater ITO doping (e.g., a CNF : ITO ratio of 1 : 20) results in increased nanowire diameter and surface roughness, which is attributed to the higher concentration and larger size of the NIs formed upon annealing (Table 1, Figure 2 and Figure S2). As the ITO doping level is increased (i.e., CNF : ITO ratio of 1 : 30), the distribution of metal ion clusters and the resulting NIs become less localized. The large number of cross-linking sites between fibers and the higher concentration of metal ion clusters on the CNFs suggest equal accessibility to the NIs formed on different CNFs (Figure 3B). As a result, driven by the shrinkage of CNFs upon annealing, the NIs from different CNFs assemble into a spherical structure to minimize the surface energy. In the two scenarios discussed above, the metal ion clusters on the CNFs are far from saturation and form the NIs upon annealing, followed by their directed assembly and coalescence to form nanoparticles.

By contrast, when the metal ion clusters are saturated in the CNF films (e.g., a CNF : ITO ratio of 1 : 80), the ITO-conjugated CNF film resembles a solution of ITO precursors (Figure

3C). Previously, a solvothermal technique was used to produce octahedral indium oxide particles.[36] The formation of octahedral particles is due to the necessity to obtain a match between the symmetry of the crystals (i.e., octahedron) and their geometric shape. The supersaturated nature of the precursor minimizes the effect of the surface energy difference on the growth of the ITO particles, resulting in similar growth rates for the different low-index facets and the consequent formation of octahedral particles.[37] Because of this, it is not surprising that saturated ITO precursors in CNF films resulted in an octahedral morphology. Thus, no NI assembly is involved in the particle formation process.

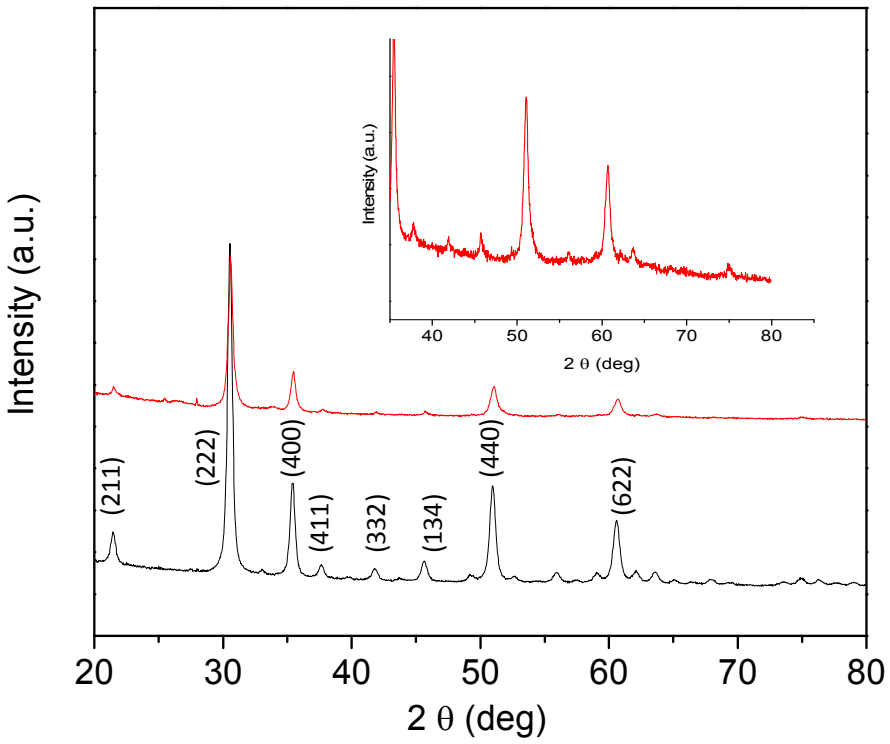

Figure 4. X-ray diffraction (XRD) spectra of commercial (black) and as-synthesized (red) indium tin oxide (ITO) nanoparticles (cellulose nanofibril : ITO ratio of 1 : 20). Inset: Zoomed-in view of the XRD spectrum of ITO nanowire in the 2θ range of 35 to 80.

Preparation of ITO thin films. Given that the morphology of an ITO film plays an important role in its performance in various devices, synthesis of ITO films with tunable morphologies

may contribute to a better understanding of the structure-property-performance relationship for improved device performance. Thus, we next sought to adapt this templating technology to prepare ITO coatings on glass slides. As mentioned previously, dilute CNF and ITO precursor solutions are necessary to limit nanoparticle aggregation. In contrast, to prepare ITO coatings, concentrated solutions were used to prepare the ITO precursor-conjugated CNF films, which were then placed on a glass slide and sintered at elevated temperatures to form ITO coatings (Supporting Information). Among films with different morphologies, films yielded from octadedral particles exhibited the best electrical properties. As shown in **Figure 5**, the particles (i.e., octahedrons) coalesce to form a continuous film that is characterized by a close-packed geometry. The resulting ITO film exhibited great transparency (~80%) in the visible light range and, low resistivity (3.8×10^{-3} Ω/cm) as estimated by the Hall effect measurement.

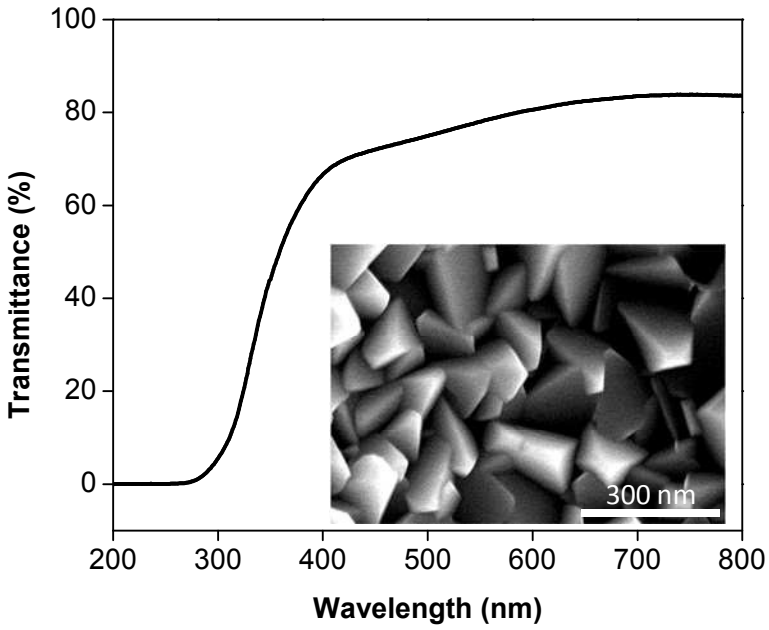

Figure 5. Transmittance of the indium tin oxide (ITO) coating formed by octahedral nanoparticles. Inset: Scanning electron microscopy image of the ITO coating.

Of note, the thickness used in the Hall effect measurement was determined using a scanning electron microscope image (Figure S3). The sheet resistance was found to be 150 Ω/□ using a four-point technique. The optical and electrical properties of the ITO coating prepared by the nanocellulose-template method indicate that it is suitable for transparent conductive oxide applications,[38, 39] demonstrating the great potential of this technique as an alternative to physical deposition. Indeed, the resistivity of this ITO film is comparable to that of films prepared using radio frequency magnetron sputtering.[39] Further improvement of the properties of these materials may be accomplished by synthesizing ITO particles with smaller diameters or better packing density.

Conclusions

We developed a unique technique to prepare ITO nanoparticles and thin films using CNF templates that facilitate control of the spatial distribution of the ITO precursors. To the best of our knowledge, this is the first report on the study of synthesizing metal oxide nanostructures with controlled morphologies using CNF templates. The templating route presented in this work is a novel, scalable, and environmentally friendly approach to prepare common metal oxide nanoparticles and thin films. We are currently investigating the performance of ITO films with tunable morphologies in transparent electronics. We are exploring the tunability of the particle size using this technique. In addition, we are exploring the use of this templating technique to form n- and p-type metal oxide interpenetrating networks.

Acknowledgments

This research was sponsored by the Laboratory Directed Research and Development Program of Oak Ridge National Laboratory, managed by UT-Battelle, LLC, for the US Department of Energy. The authors also wish to acknowledge the support of the US Department of Agriculture Forest Products Laboratory and its staff.

References

1. Z. L. Shen, P. E. Burrows, V. Bulovic, S. R. Forrest and M. E. Thompson, *Science*, 1997, **276**, 2009-2011.
2. H. T. Ng, A. P. Fang, L. Q. Huang and S. F. Y. Li, *Langmuir*, 2002, **18**, 6324-6329.
3. Y. J. Cho, T. K. Ahn, H. Song, K. S. Kim, C. Y. Lee, W. S. Seo, K. Lee, S. K. Kim, D. Kim and J. T. Park, *J. Am. Chem. Soc.*, 2005, **127**, 2380-2381.
4. J. T. Mccue and J. Y. Ying, *Chem. Mater.*, 2007, **19**, 1009-1015.
5. K. R. Wu and T. P. Cho, *Appl. Catal., B*, 2008, **80**, 313-320.
6. J. Q. Hu, F. R. Zhu, J. Zhang and H. Gong, *Sens. Actuators, B*, 2003, **93**, 175-180.
7. Q. H. Wu, *Crit. Rev. Solid State Mater. Sci.*, 2013, **38**, 318-352.
8. T. Brezesinski, J. Wang, J. Polleux, B. Dunn and S. H. Tolbert, *J. Am. Chem. Soc.*, 2009, **131**, 1802-1809.
9. Y. J. Liu, G. Stefanic, J. Rathousky, O. Hayden, T. Bein and D. Fattakhova-Rohlfing, *Chem. Sci.*, 2012, **3**, 2367-2374.
10. J. Lee, S. Lee, G. L. Li, M. A. Petruska, D. C. Paine and S. H. Sun, *J. Am. Chem. Soc.*, 2012, **134**, 13410-13414.
11. L. Alibabaei, B. H. Farnum, B. Kalanyan, M. K. Brennaman, M. D. Losego, G. N. Parsons and T. J. Meyer, *Nano Lett.*, 2014, **14**, 3255-3261.
12. H. B. Yao, G. Y. Zheng, P. C. Hsu, D. S. Kong, J. J. Cha, W. Y. Li, Z. W. Seh, M. T. McDowell, K. Yan, Z. Liang, V. K. Narasimhan and Y. Cui, *Nat. Comm.*, 2014, **5**, 3943.
13. P. C. Yu, C. H. Chang, M. S. Su, M. H. Hsu and K. H. Wei, *Appl. Phys. Lett.*, 2010, **96**, 153307.
14. S. I. Choi, K. M. Nam, B. K. Park, W. S. Seo and J. T. Park, *Chem. Mater.*, 2008, **20**, 2609-2611.
15. N. Du, H. Zhang, B. D. Chen, X. Y. Ma, Z. H. Liu, J. B. Wu and D. R. Yang, *Adv. Mater.*, 2007, **19**, 1641-1645.
16. S. Y. Xu and Y. Shi, *Sens. Actuators, B*, 2009, **143**, 71-75.
17. E. N. Dattoli and W. Lu, *MRS Bull.*, 2011, **36**, 782-788.
18. S. T. Li, X. L. Qiao, H. G. Chen, H. S. Wang, F. Jia and X. L. Qiu, *J. Cryst. Growth*, 2006, **289**, 151-156.
19. H. Usui, T. Sasaki and N. Koshizaki, *J. Phys. Chem. B*, 2006, **110**, 12890-12895.
20. J. H. Ba, D. Fattakhova-Rohlfing, A. Feldhoff, T. Brezesinski, I. Djerdj, M. Wark and M. Niederberger, *Chem. Mater.*, 2006, **18**, 2848-2854.
21. J. Ba, A. Feldhoff, D. Fattakhova-Rohlfing, M. Wark, M. Antonietti and M. Niederberger, *Small*, 2007, **3**, 310-317.
22. P. S. Devi, M. Chatterjee and D. Ganguli, *Mater. Lett.*, 2002, **55**, 205-210.
23. C. Q. Zhu and M. J. Panzer, *Chem. Mater.*, 2014, **26**, 2960-2966.
24. X. T. Zhang, Z. Liu, Y. P. Leung, Q. Li and S. K. Hark, *Appl. Phys. Lett.*, 2003, **83**, 5533-5535.
25. H. Imai, Y. Takei, K. Shimizu, M. Matsuda and H. Hirashima, *J. Mater. Chem.*, 1999, **9**, 2971-2972.
26. J. T. Korhonen, P. Hiekkataipale, J. Malm, M. Karppinen, O. Ikkala and R. H. A. Ras, *ACS Nano*, 2011, **5**, 1967-1974.
27. W. Czaja, A. Krystynowicz, S. Bielecki and R. M. Brown, *Biomaterials*, 2006, **27**, 145-151.

28. W. K. Czaja, D. J. Young, M. Kawecki and R. M. Brown, *Biomacromolecules*, 2007, **8**, 1-12.
29. H. Dong, J. F. Snyder, K. S. Williams and J. W. Andzelm, *Biomacromolecules*, 2013, **14**, 3338-3345.
30. Y. Habibi, L. A. Lucia and O. J. Rojas, *Chem. Rev.*, 2010, **110**, 3479-3500.
31. I. Siro and D. Plackett, *Cellulose*, 2010, **17**, 459-494.
32. M. Niederberger, *Acc. Chem. Res.*, 2007, **40**, 793-800.
33. I. Ichinose, H. Senzu and T. Kunitake, *Chem. Mater.*, 1997, **9**, 1296-1298.
34. F. Ivaldi, N. A. K. Kaufmann, S. Kret, A. Dussaigne, B. Kurowska, M. Klepka, J. Dabrowski, P. Dluzewski and N. Grandjean, *17th International Conference on Microscopy of Semiconducting Materials 2011*, 2011, **326**.
35. A. Volmer and A. Weber, *Physik. Chem.*, 1926, **119**, 277-301.
36. W. Zhang, Z. Huang, T. Li, Q. Tang, D. K. Ma and Y. T. Qian, *Chem. Lett.*, 2005, **34**, 118-119.
37. M. Wei, D. Zhi and J. L. MacManus-Driscoll, *Nanotechnology*, 2006, **17**, 3523-3526.
38. T. Minami, *Semicond. Sci. Technol.*, 2005, **20**, S35-S44.
39. V. S. Reddy, K. Das, A. Dhar and S. K. Ray, *Semicond. Sci. Technol.*, 2006, **21**, 1747-1752.

Table of content

Nanocellulose fibrils have been used as sacrificial templates for synthesizing ITO nanoparticles with controllable morphology.